ELSEVIER

Surface Science 412/413 (1998) 430–440

surface science

The catalytic oxidation of CO on polycrystalline Pd: experiments and kinetic modeling

Mats Eriksson *, Lars-Gunnar Ekedahl [1]

Department of Physics and Measurement Technology, Linköping University, S-581 83 Linköping, Sweden

Received 11 November 1997; accepted for publication 14 May 1998

Abstract

The catalytic oxidation of CO on a thin, polycrystalline Pd film has been studied. Even though the Pd film is expected to be dominated by (111) facets, some distinct differences compared to single crystalline Pd(111) are observed. A kinetic model for the CO oxidation reaction is presented. It gives good agreement with experiments, both in terms of CO_2 reaction probability and CO coverage during reaction conditions. The model assumes a random distribution of the adsorbates, an activation energy for the reaction that decreases with increasing CO coverage, as well as a CO sticking coefficient that in a temperature dependent fashion depends on the oxygen coverage. Single crystal data available from the literature (initial sticking coefficients and heats of adsorption) were mainly used as input parameters. Thus, the model might also be a useful starting point when modeling the catalytic oxidation of CO on single crystal surfaces.

Keywords: Carbon dioxide; Carbon monoxide; Catalysis; Models of surface chemical reactions; Oxygen; Palladium; Polycrystalline surfaces; Sticking

1. Introduction

A microscopic understanding of the CO oxidation reaction on the platinum group metals is necessary in order to understand the behavior of e.g. catalytic converters, and more specifically, chemical sensors where the catalytic metal film represents an interface towards the gas to be analyzed. We have for a long time been working with the chemistry of catalytic gas sensors, with two aims: to use sensing signals as an aid in the interpretation of reaction kinetics on catalytic surfaces; and to obtain an understanding of the sensor signals when the device is used as a chemical sensor. The experiments in this work are therefore performed on a hydrogen sensitive Pd-MOS (metal–oxide–semiconductor) structure [1]. Such a device has also been used to effectively demonstrate that e.g. CO adsorption strongly influences hydrogen adsorption [2,3], and the results presented here are related to that work. Here, both CO_2 desorption rate and CO coverage have been monitored during reaction conditions. A kinetic model for the CO oxidation reaction is presented, combining new results with previously published data for single crystalline surfaces, aiming at further insight into the adsorption properties of CO on oxygen covered transition metal surfaces.

The oxidation of CO on the platinum group metals has been studied extensively in the past. For

* Corresponding author. Fax: +46 13 288969; e-mail: maeri@ifm.liu.se

[1] Formerly Petersson.

0039-6028/98/$ – see front matter
PII: S0039-6028(98)00462-2

instance, Ertl and coworkers have shown that the oxidation of CO on Pd(111), (100) and (110) single crystals as well as on polycrystalline wires proceeds via a Langmuir–Hinshelwood (L–H) mechanism in the sense that both reactants must be chemisorbed before reaction can take place, and that the reaction rate is not strongly structure sensitive [4–6]. Goschnick et al. later showed that the microscopic details are different on Pd(110) than on Pd(111), but the overall rates are nearly identical due to a compensation effect [7]. The L–H mechanism has also been confirmed by Matsushima in the case of a polycrystalline Pd foil [8].

The effect of adsorbed oxygen on the CO adsorption rate is an important part of the problem. An interesting difference between Pd(111) [4] and Pt(111) [9], studied by Ertl and coworkers for similar conditions, was that the CO_2 production rate decreased with increasing oxygen coverage at high temperatures on Pt(111) but not on Pd(111). In this paper we will show that a similar decrease of the CO_2 production rate with increasing oxygen coverage may also occur in the case of polycrystalline Pd even though the Pd film is dominated by (111) facets. Previously, we have demonstrated that a similar process occurs on a SiO_2 supported Pd model catalyst, although CO and oxygen spillover also seems to be important in that case [10].

A low energy electron diffraction (LEED) study by Conrad et al. revealed that, at 300 K, the adsorption behavior of CO, on an oxygen saturated Pd(111) surface, was dependent on the CO pressure [5]. At $p_{CO} \approx 1 \times 10^{-7}$ Torr, the LEED data suggests that a build up of CO coverage along with a compression of the oxygen adlayer occurs before an appreciable reaction between the adsorbates takes place. This was consistent with the results of a molecular beam study [4]. At $p_{CO} \approx 1 \times 10^{-8}$ Torr, the LEED data instead indicates that no compression occurs and that the CO coverage increases parallel with a consumption of the adsorbed oxygen. The present work deals with the lower CO pressure range.

2. Experimental details

The experiments were carried out in an ultra-high vacuum (UHV) chamber equipped with two mass spectrometers for detection of desorbing products and control of the background partial CO pressure during CO_2 production, respectively. Facilities for electron energy loss spectroscopy (EELS), ultraviolet photoelectron spectroscopy (UPS) and surface potential measurements were also available.

All pressures and exposures given in this paper have been calculated from the readings of a hot cathode pressure gauge by dividing by the sensitivity factors tabulated by Nakao [11], i.e. 0.87 for O_2 and 1.0 for CO. Our experience is that this gives true pressures, accurate to within 10% of a stated value.

The samples were fabricated in the form of a Pd-MOS structure. Such a device has the advantage of acting as a very sensitive hydrogen detector [12], although this property is not specifically utilized in this work. The SiO_2 thickness was 100 nm, obtained by oxidation of a Si wafer at 1200°C in dry oxygen. Immediately after oxidation, the support was transferred to a vacuum chamber where Pd was electron beam evaporated onto the oxide at room temperature. The pressure was below 8×10^{-7} Torr during the evaporation. The Pd thickness was 100 nm, as determined by a quartz micro balance, and the size of the Pd covered area was 8×8 mm^2. Two samples from the same batch were used in the study. One was used during the EELS measurements and was transferred into the UHV chamber with a load-lock system. The second sample, used for the rest of the measurements, was inside the UHV chamber during bake-out at 450 K. Both samples were cleaned by mild Ar sputtering ($V_{beam} = 500$ V, $J_{Ar^+} \approx 1$ μA cm^{-2}) followed by alternating O_2 and H_2 exposures at temperatures between 473 and 573 K, which we know from earlier experience produces a clean Pd surface [13,14]. For example, the valence band spectrum recorded with UPS shows no indication of contamination. The shape of the H_2O production rate versus time, during hydrogen titration of an oxygen precovered surface, is also a sensitive probe that was used to check the cleanliness of the Pd surface [15]. The work function change of the Pd film for a 6 L O_2 exposure was 430 meV and close to saturation, which also indicates a clean sample

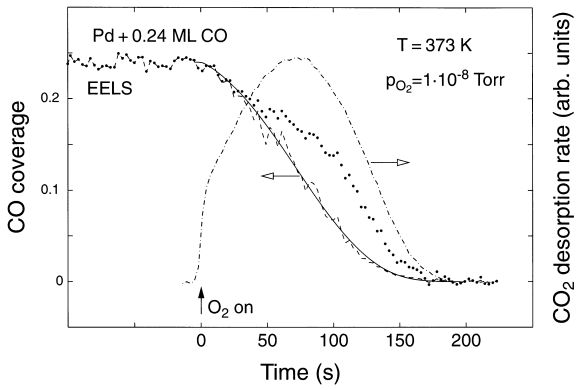

Fig. 1. Calibration of the EELS intensity. A CO precovered surface is titrated with oxygen, while the CO_2 desorption rate (dashed–dotted line) and EELS intensity (dotted) are simultaneously measured. From the CO_2 desorption rate, the CO coverage as a function of time was evaluated (solid line). By fitting a mathematical expression, the EELS intensity could be transformed to CO coverage (dashed line).

($1\ \mathrm{L} = 1 \times 10^{-6}$ Torr s). No differences between the two samples were observed in any experiment. The base pressure during the measurements was in both cases around 5×10^{-11} Torr. Previous TEM studies of similarly treated structures have revealed that the Pd films have grains with diameters of several hundred nanometers and that the (111) orientation dominates [16].

EELS studies were performed in order to follow the variation of the CO coverage during the catalytic CO_2 reaction. The energy resolution in this case (around 30 meV) did not allow studies of site related energy shifts. In these experiments the energy was locked at the CO induced energy loss, located at a loss energy of 240 meV below the elastic peak. In order to minimize the dependence of the EELS signal to a varying oxygen coverage, these measurements were performed with the Pd surface 9° off the specular reflection. Fig. 1 shows the variation of the EELS intensity during titration of a CO pre-exposed surface with oxygen. From the CO_2 production rate, which was simultaneously followed by a mass spectrometer, the variation of the CO coverage with time can be plotted (assuming that the CO desorption is negligible in this time interval). As seen in the figure, the EELS intensity is not directly proportional to the CO coverage. By fitting a mathematical expression to the EELS data, a transformation can, however, be made to improve the agreement. In this case the initial CO coverage was 0.24 ML. Above this coverage, we use the EELS intensity as a direct measure of the CO coverage, since titration at these CO coverages was difficult to perform. It is the transformed version of the EELS signal that is shown in the figures below.

In order to be able to perform EELS, the sample had to be moved away from the mass spectrometer, so the simultaneously measured mass spectrometer signals were less intense than otherwise. It was, however, clear that the shape of the CO_2 productions during the EELS measurements was equal to those obtained with the sample facing the mass spectrometer.

The model calculations were performed with the ode15s differential equation solver in the MATLAB program package.

3. Results and discussion

3.1. Combustion of CO on an oxygen precovered Pd surface

The experiments described in this section were performed in the following manner. The sample was first exposed to a certain dose of oxygen and then to CO at constant temperature and pressure while recording the CO_2 production rate and/or the EELS intensity at the CO induced peak. The background contribution of the mass spectrometer signal, which was mainly a slowly drifting signal due to the oxygen pre-exposure, has been subtracted in the figures. The oxygen and CO saturation coverages are defined as $\theta_O = 0.25$ ML and $\theta_{CO} = 0.5$ ML, respectively, with the monolayer (ML) concentration assumed to be equal to that of Pd(111), $1.5 \times 10^{19}\ \mathrm{m}^{-2}$. These values are in accordance with published data [5,17,18].

Fig. 2 shows the results for an initial oxygen exposure of 11.5 L O_2, corresponding to an oxygen coverage of 0.22 ML. A first and very crude model that can be compared with these data is obtained by assuming that the reactivity of all incoming CO molecules is equal to unity. This is shown by the full line in Fig. 2.

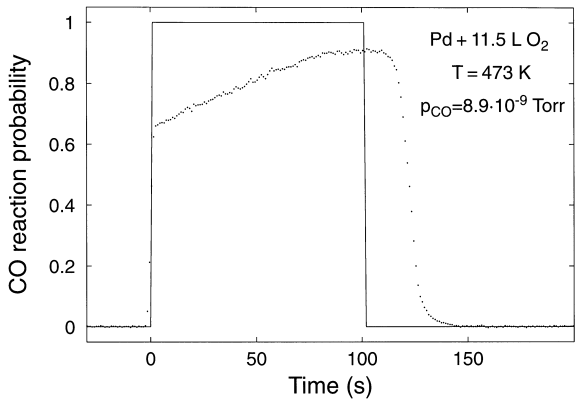

Fig. 2. The measured CO_2 desorption rate (dotted) during CO exposure of an oxygen precovered Pd surface. The solid line shows a hypothetical reaction with reaction probability 1 and the same impingement rate as the CO molecules. The graphs are drawn with equal areas.

Since the areas below the graphs in Fig. 2 are plotted equal for both the CO_2 production and the hypothetical reaction (i.e. corresponding to equal amounts of preadsorbed oxygen), the experimental CO reaction probability is directly given by the value on the abscissa in Fig. 2. (The CO reaction probability is defined as the ratio between the CO_2 production rate and the incoming flux, r_{CO_2}/F_{CO}.) It is thus seen that the maximum reaction probability for CO is 0.9 at 473 K, with an estimated error within 10% due to the uncertainty in the ion gauge pressure value. Clearly, at this temperature the model assuming a reaction probability equal to unity is not at all a bad approximation. The most obvious discrepancy is seen for the high oxygen coverages, suggesting that oxygen (weakly) affects the reactive sticking coefficient of CO. Lowering the temperature will, however, severely change the reaction probabilities, probably as a consequence of increased CO adsorption.

In Fig. 3a the CO reaction probability versus time is plotted for five different temperatures. The initial oxygen exposure was 11.5 L O_2 and the CO pressure 8.9×10^{-9} Torr. The initial oxygen coverage is, for each temperature, close to 0.22 ML. It is seen that, for the three highest temperatures, the CO_2 desorption rate increases initially approximately linearly with time (and thus decreasing oxygen coverage). The CO_2 desorption rate at

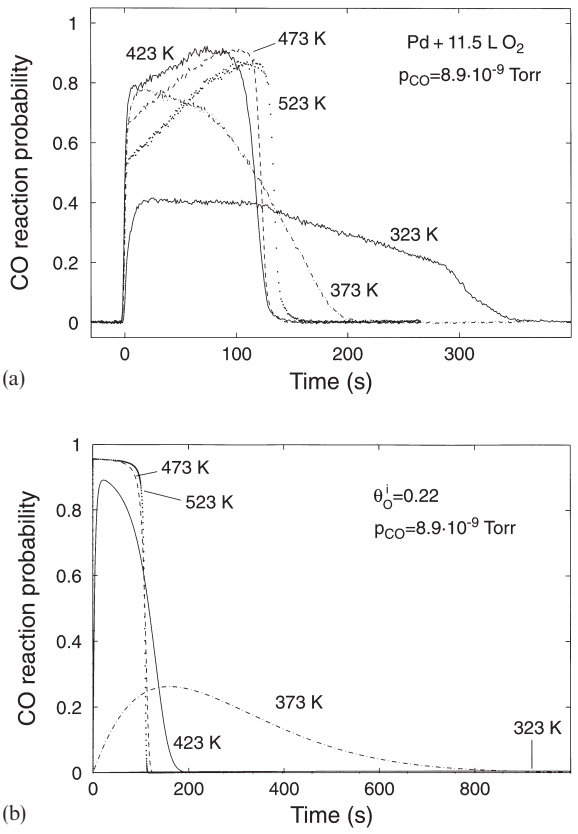

Fig. 3. (a) Measurements of the CO_2 production rate during CO exposure of an oxygen precovered Pd surface for different temperatures. (b) The "simple model" (see text) applied to the conditions in (a). Note the difference in time scale.

373 K is initially higher than at 473 and 523 K, but decreases with time. At 323 K the CO_2 desorption rate is much lower and, furthermore, the increase of the rate upon CO turn on is slower than at higher temperatures.

As a comment to Fig. 3a, it should be mentioned that a similar oxygen induced effect on the sticking coefficient of CO was not observed on Pd(111) [4], but could, on the other hand, be seen for similar conditions on Pt(111) [9] and on Pd(110) [7]. Matsushima and White [19] concluded from an Auger electron spectroscopy study of a Pd foil that the CO reaction probability was independent of both temperature and oxygen coverage in the temperature interval $458 < T < 720$ K. An explana-

tion of these differences is possibly that surface structure is important.

The rate equations for a simple L–H type of reaction may be written as:

$$r_{CO_2} = \frac{d[CO_2]}{dt} = \alpha\theta_{CO}\theta_{CO}N_s, \quad (1)$$

$$\frac{d\theta_{CO}}{dt} = \frac{F_{CO}S^0_{CO}}{N_s}(1-2\theta_{CO}) - \epsilon\theta_{CO} - \alpha\theta_{CO}\theta_O, \quad (2)$$

$$\frac{d\theta_O}{dt} = -\alpha\theta_{CO}\theta_O, \quad (3)$$

where r_{CO_2} is the CO_2 desorption rate, $F_{CO} = N_A p_{CO}/\sqrt{2\pi M_{CO} R T_{gas}}$ the impingement rate of CO molecules ($m^{-2}\,s^{-1}$), S^0_{CO} the CO sticking coefficient on the clean Pd surface (0.96 [20]) and N_s the concentration of adsorption sites ($1.5\times10^{19}\,m^{-2}$). ϵ and α are Arrhenius expressions of the form $\nu e^{-\Delta H/k_B T}$, where ν is a prefactor and ΔH an activation barrier. The three terms of Eq. (2) represent adsorption, desorption and reaction contributions, respectively. The adsorption is assumed to be blocked by CO molecules adsorbed on the surface, but not by adsorbed oxygen atoms. In Fig. 3b the reactions are simulated according to Eqs. (1)–(3), using a constant activation barrier for CO_2 formation, $\Delta H_{CO_2} = 1.09$ eV [4].

When comparing Fig. 3a and b it is immediately clear that this simulation is too simple to describe the observed data, even if another value of ΔH_{CO_2} were chosen, a conclusion also drawn in the case of a single crystalline Pd(111) surface [4,5]. It is also obvious that adding a simple oxygen blocking in the CO adsorption term would not be enough to describe the observed trends, since a clear temperature dependence is observed also for the high temperatures at equivalent oxygen coverages. Furthermore, it seems quite clear that the activation energy for CO_2 formation, ΔH_{CO_2}, must be reduced in the low temperature case where both CO and oxygen are coadsorbed, in order to account for the larger experimental reaction rates.

In Fig. 4a and b, the CO_2 desorption rates vs. time for different initial oxygen exposures are shown for two different temperatures, respectively. Clearly, for $T = 523$ K (Fig. 4a) the CO_2 production is a single valued function of the oxygen coverage. Independent of the initial oxygen coverage, it takes around 5 s to reach the equilibrium production rate, which is equal to the time it took to reach the desired CO pressure and after which the CO partial pressure was held constant, within 1%. At $T = 323$ K (Fig. 4b), however, the CO_2 desorption rate increases much more slowly than the CO partial pressure, indicating that a CO coverage is built up before the equilibrium rate is obtained. This is particularly obvious at low initial oxygen coverage, since then a larger CO coverage will have to be formed before equilibrium conditions are reached. We will refer to the time interval before equilibrium conditions are reached as the "induction period". For $T \geq 423$ K the CO_2 desorp-

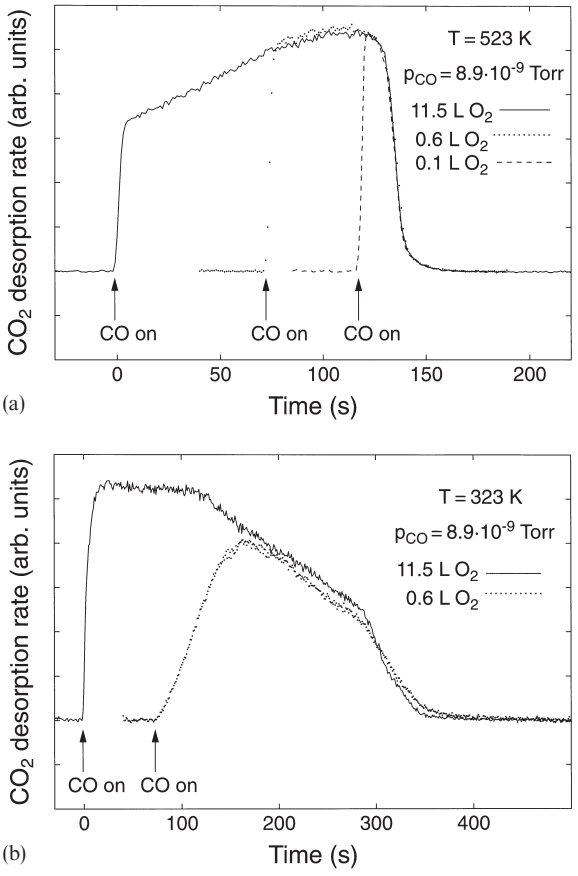

Fig. 4. CO_2 production rate during CO exposure of Pd surfaces with different initial oxygen coverages at $T = 523$ K (a) and $T = 323$ K (b). Note the different time scales in (a) and (b).

tion rate was always a single valued function of oxygen coverage, indicating that there is no build up of a substantial CO coverage during the reaction at these temperatures and pressures. This further confirms that the decrease of r_{CO_2} with increasing oxygen coverage, observed at $T \geq 423$ K, is indeed due to a lowered CO sticking coefficient at high oxygen coverages.

In their investigations on Pd(111), Ertl and coworkers observed an induction period at low temperatures, during which a build up of a CO coverage was simultaneously observed [4,5]. In that case the induction period was even more pronounced than in our case, and a compression of the oxygen adlayer could be detected with LEED for relatively high CO pressures and low temperatures [5]. The LEED data indicated, furthermore, that the compression effect was absent if the CO pressure was low. A difference between this study and the study performed by Ertl and coworkers (apart from the surface structure) is that we have used a much lower CO pressure, which is then consistent with the less pronounced induction period in our case. The induction period observed in our case is thus only due to the build up of a CO coverage and not to any compression of the oxygen adlayer. It is, however, likely that the induction period in our experiments is slightly affected by adsorption of a small amount ($\theta_{CO} < 0.05$ is estimated) of CO from the background during the lowering of the temperature to 323 K and the subsequent oxygen exposure.

In order to facilitate a proper modeling of the CO_2 production rate, the CO coverage was measured with EELS during the CO_2 production. The results are shown in Fig. 5. The CO coverage is obtained from the EELS signal as described in Section 2. The oxygen coverage is calculated from the CO_2 desorption rate:

$$\frac{d\theta_O}{dt} = -\frac{d[CO_2]}{dt}\alpha_{CO_2} \quad (4)$$

where α_{CO_2} is a calibration constant. These measurements show that the CO coverage is negligible during the CO_2 production for $T > 423$ K. For $T < 423$ K a build up of CO coverage during the reaction is observed which is quite substantial at $T = 323$ K.

Since the CO coverage is negligible during the CO_2 production for $T > 423$ K, the low initial CO_2 production rate must be due to a lowered CO sticking. This lowering increases with increasing temperature. For Pt(111) this was explained by capture of impinging CO molecules in a precursor state above the oxygen adlayer. From this state the CO molecule either desorbs or adsorbs (possibly followed by reaction). When the oxygen coverage is lowered, the CO sticking coefficient approaches the value on the clean Pt surface. It is reasonable that the same effect is observed in our case. As stated previously, this phenomenon was, however, not observed on Pd(111) [4]. It may seem strange that our Pd data resembles more the data obtained from Pt(111) than from Pd(111), but possibly in this region of oxygen coverage the reaction is more sensitive to structural defects than to the chemical composition of the substrate. This is not unreasonable, if one accepts the CO adsorption precursor model, since in such a case, the initial adsorption occurs on the oxygen covered parts of the surface, and thus could be less sensitive to the chemical composition of the underlying substrate.

3.2. Kinetic modeling

The simple modeling shown in Fig. 3b is mainly lacking in its ability to describe two things:

(i) the variation of the CO sticking coefficient with oxygen coverage and temperature;

(ii) the apparent decrease of the activation barrier for CO_2 formation at low temperatures, where CO and oxygen are coadsorbed on the surface.

We will now improve the model by considering a case where the oxygen atoms are randomly distributed on the surface. Since the mobility of CO is much larger than that of oxygen on Pd, we consider the adsorbed CO molecules to move in a static framework of the oxygen atoms. An impinging CO molecule is expected to be trapped in a precursor state before chemisorption. The desorption from this precursor state is influenced by the oxygen coverage. Furthermore, the CO–CO inter-

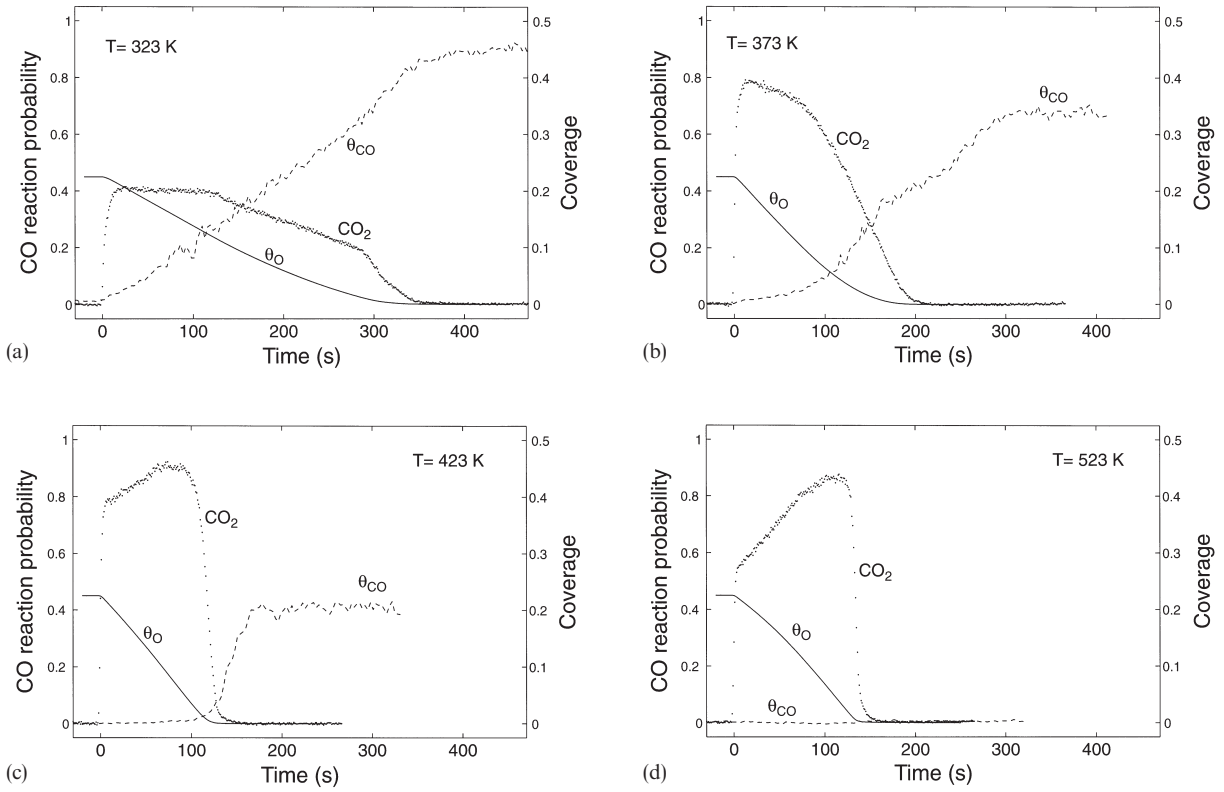

5

Fig. 5. Measurements of the variation of θ_{CO}, θ_O and the CO_2 production rate versus time during CO exposure of an oxygen precovered surface for $T=323$ K, $T=373$ K, $T=423$ K and $T=523$ K. The CO_2 desorption rate curves are taken from Fig. 3a. $p_{CO}=8.9\times10^{-9}$ Torr.

action is assumed to influence the activation energy for the $CO_{ad}+O_{ad}\rightarrow CO_2$ reaction step.

The dependence of the CO sticking coefficient on the coverages of oxygen and CO is modeled by

$$S_{CO}=S^0_{CO}[1-\nu_{app}\,e^{-\Delta H_{app}/k_BT}4\theta_O-(2\theta_{CO})^3]. \quad (5)$$

The oxygen coverage dependent term approximates the reduction of the CO sticking coefficient due to desorption from the precursor state. ν_{app} and ΔH_{app} are the apparent prefactor and the desorption energy of the precursor state, respectively. The CO coverage dependent term is included to mimic the adsorption of CO on Pd(111), as observed by Engel in the absence of oxygen on the surface [20]. In the case of Pd(111) the decrease of S_{CO} with increasing CO coverage was observed to be less than linear. A more physically correct description of this dependence would perhaps be to use a Kisliuk type of expression [20–22], but mathematically our simple description is a good approximation. $S^0_{CO}=0.96$ was concluded in the case of Pd(111) and is used in the modeling [20]. At the temperatures and pressures of our investigation, a maximum CO coverage of 0.5 ML is expected [5]. On Pd(110) it has been observed that an adsorbed oxygen atom may block more than 10 adsorption sites [23]. We have not observed such a blocking behavior on the CO sticking coefficient.

Engels also observed that the CO adsorption energy decreases approximately linearly with CO coverage:

$$\Delta H_{CO}=\Delta H^0_{CO}(1-a\theta_{CO}) \quad (6)$$

where $\Delta H^0_{CO} = 1.4$ eV and $a = 0.45$ [20].

In our model we assume that it is the local CO coverage, i.e. the CO concentration scaled to the concentration of sites not occupied by oxygen, that determines the CO adsorption energy:

$$\Delta H_{CO} = \Delta H^0_{CO}\left(1 - a\frac{\theta_{CO}}{1-4\theta_O}\right). \quad (7)$$

The reason for this is that the sites occupied by adsorbed oxygen are not available for adsorbed CO, only for reaction. Since the activation barrier for CO diffusion is much lower than the reaction barrier, the CO molecules will spend most of the surface residence time moving between sites not occupied by oxygen. Thus, for a certain CO coverage, the CO–CO interaction will increase with increasing oxygen coverage and we take Eq. (7) as a reasonable representation of this. It has been shown that the oxygen adsorption energy might also be reduced when CO and oxygen are coadsorbed at high total coverage [4,5]. We have neglected such effects in the modeling.

The reduction of ΔH_{CO} will also lead to a reduction of the activation energy barrier for CO_2 formation, ΔH_{CO_2}. According to the theory of bond order conservation, developed by Shustorovich [24,25], ΔH_{CO_2} can be calculated from:

$$\Delta H_{CO_2} = \frac{\Delta H_{CO}\Delta H_O}{\Delta H_{CO} + \Delta H_O}. \quad (8)$$

If we use the low coverage values $\Delta H^0_{CO} = 1.4$ eV and $\Delta H_O = 3.78$ eV (the oxygen atomic chemisorption energy) we obtain $\Delta H_{CO_2} = 1.02$ eV, which is in good agreement with the experimentally observed low coverage value of 1.09 eV [4].

Thus, we end up with a set of rate equations similar to Eqs. (1)–(3) but where Eq. (2) is replaced with Eq. (9):

$$\frac{d\theta_{CO}}{dt} = \frac{F_{CO}S^0_{CO}}{N_s}[1 - v_{app}\, e^{-\Delta H_{app}/k_B T}4\theta_O - (2\theta_{CO})^3] - \epsilon\theta_{CO} - \alpha\theta_{CO}\theta_O \quad (9)$$

and where the rate constants and activation energies are now defined in the following way:

$$\alpha = v_{CO_2}\, e^{-\Delta H_{CO2}/k_B T},$$

$$\epsilon = v_{CO}\, e^{-\Delta H_{CO}/k_B T},$$

$$\Delta H_{CO} = \Delta H^0_{CO}\left(1 - a\frac{\theta_{CO}}{1-4\theta_O}\right),$$

and

$$\Delta H_{CO_2} = \frac{\Delta H_{CO}\Delta H_O}{\Delta H_{CO} + \Delta H_O}.$$

The values of the constants are listed in Table 1.

The result of the modeling is shown in Fig. 6. A considerable improvement compared to the simple model presented in Fig. 3b is achieved. Compared to the experimental results, it is clear that all trends are well described, both for the CO_2 production rate (reaction probability) and the variation of the CO coverage. The agreement is not perfect but can be improved with a more advanced model, e.g. by introducing a variation of the oxygen adsorption energy. Also, the rather abrupt changes of the slope of the desorption rate curves, that might indicate different oxygen phases, cannot be described with our relatively simple model. A more detailed modeling would, however, be meaningful only if we had a more detailed knowledge of e.g. the adsorbate structure and energetics than we presently have. One model that we have considered is the oxygen island model described by Hellsing and Zhdanov [26]. The agreement with experimental data in that case was, however, not as good as that of Fig. 6.

Table 1
Constants used in the model calculations

Parameter	Value	Unit
ΔH^0_{CO}	1.4	eV
ΔH_O	3.78	eV
a	0.45	—
v_{CO}	1×10^{13}	$m^{-2}\,s^{-1}$
v_{CO_2}	1×10^{13}	$m^{-2}\,s^{-1}$
v_{app}	11	—
ΔH_{app}	0.14	eV
N_s	1.5×10^{19}	m^{-2}

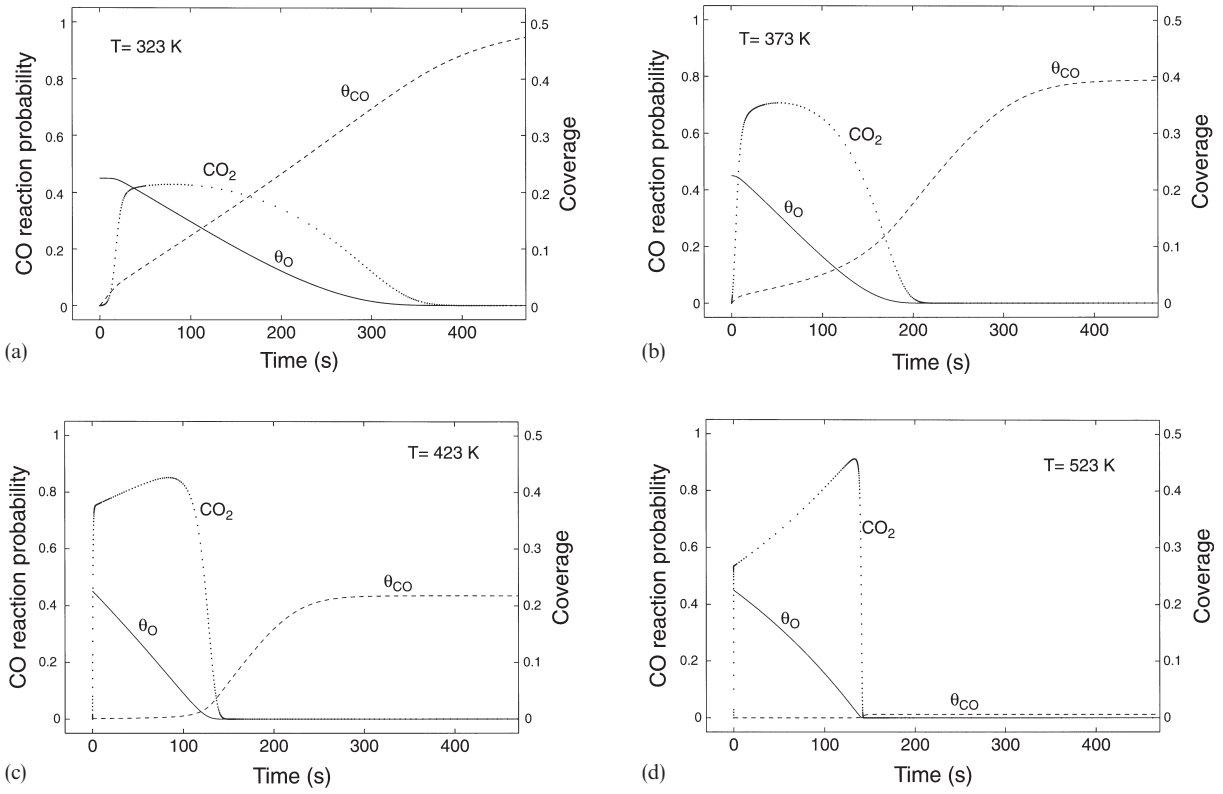

Fig. 6. Modeling of the variation of θ_{CO}, θ_O and the CO_2 production rate versus time during CO exposure of an oxygen precovered surface, for the same conditions as in the experiments presented in Fig. 5.

3.3. Application to CO pulses in an oxygen atmosphere

An instructive way to look at the CO–oxygen reaction is to study the CO_2 desorption rate during an experiment where the surface is exposed to CO pulses at various pressures in a constant oxygen atmosphere. Such an experiment is shown in Fig. 7 for $T=473$ K. The oxygen exposure between the CO pulses is 0.6 L, which means that $\theta_O \approx 0.12$ ML when the CO pulses are turned on. Clearly, two regions will exist, one where the CO pressure is high enough so that CO may consume all preadsorbed oxygen, and one where this is not the case. For the three highest CO pressures of Fig. 7 the steady state CO_2 production is indeed preceded by a higher production rate, due to consumption of most of the accumulated oxygen. The maximum rate, in that part of the CO_2 pro-

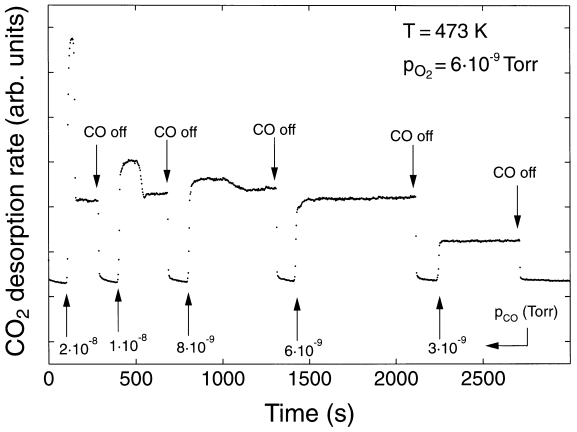

Fig. 7. CO_2 desorption rate during CO pulses in an atmosphere of oxygen. In this figure no background subtractions have been made.

duction, is approximately proportional to the CO pressure, as would be expected from our model. The steady state rate, however, is slightly decreasing with increasing CO pressure, probably due to a build up of a small CO coverage that inhibits O_2 dissociation. The maximum steady state rate was observed for $p_{CO}=7\times10^{-9}$ Torr in a separate "close-up" experiment. In that case no preceding maximum occurred. For CO pressures lower than 7×10^{-9} Torr, the steady state production decreases approximately proportionally to the CO pressure, since now the CO flux is rate limiting and the dependence on the oxygen coverage at $T=473$ K is small.

$p_{CO}/p_{O_2}=7/6$ thus defines a critical pressure ratio, at which the CO_2 steady state production rate is at maximum. Above the critical ratio CO is in excess at the surface, and below it oxygen is. However, if, at steady state production in the CO excess region, the CO pressure was rapidly increased from 8×10^{-9} Torr to 2.5×10^{-8} Torr, a transient increase in the CO_2 desorption rate was observed before the new steady state was reached. This clearly demonstrates that a small but significant oxygen coverage exists at steady state production, also above the critical pressure ratio.

Assuming that the CO desorption is negligible (valid for $\theta_O\geq0.02$ ML), the oxygen coverage at the critical ratio can roughly be estimated since at steady state production all incoming molecules that stick on the surface end up as CO_2. The flux of molecules hitting the surface is, at constant temperature, proportional to $p/\sqrt{M}$, where p is the applied partial pressure and M is the molecular weight. This means that at steady state:

$$2\frac{p_{O_2}}{\sqrt{M_{O_2}}}S_{O_2}=\frac{p_{CO}}{\sqrt{M_{CO}}}S_{CO}. \quad (10)$$

The oxygen sticking is given by $S_{O_2}=S^0_{O_2}(1-4\theta_O)^2$, with $S^0_{O_2}=0.8$ [10] and S_{CO} by Eq. (5). Note that the CO coverage at this temperature and pressure is low ($\theta_{CO}\approx0.07$ ML on the oxygen free surface) so that it will not influence any of the sticking coefficients. Utilizing the result of our model (and Table 1) with $p_{CO}=7\times10^{-9}$ Torr and $p_{O_2}=6\times10^{-9}$ Torr at $T=473$ K then gives $\theta_O=0.04$ ML. Thus, maximum CO_2 production at steady state is obtained when the surface carries an oxygen coverage of around 0.04 ML.

This value also corresponds to maximum CO_2 production in the titration experiments in Fig. 3a and is consistent with the observation that the CO_2 production rate decreases sharply at low oxygen coverage. In the limit of low coverages of both CO and oxygen, the CO desorption probability becomes larger than the reaction probability with oxygen.

An experiment, similar to that of Fig. 7, performed at 373 K showed that, during consumption of the adsorbed oxygen, a CO coverage was built up which caused the CO_2 production rate to decrease drastically. The reason for this is the low CO desorption rate at 373 K and the well known inhibition of oxygen adsorption on a CO covered Pd surface.

4. Conclusions

The here proposed model for the catalytic oxidation of CO on polycrystalline Pd gives good agreement with experiments, both in terms of CO_2 reaction probability and CO coverage during reaction conditions. Single crystal data (initial sticking coefficients and heats of adsorption) were mainly used as input parameters. Thus, a similar model might also be a useful starting point when modeling the catalytic oxidation of CO on a single crystal surface.

The observed CO_2 production rate can be described by a simple rate law and is proportional to the product of the oxygen and the CO surface coverage. This is in contrast to observations on single crystal Pd(111) and Pd(110) where segregation of the reactants is proposed to dominate the reaction behavior [4,7]. The rate constant increases with CO coverage through a decrease of the activation energy of the process. The activation energy is derived from the heats of adsorption for oxygen (which is here treated as a constant) and CO. Thus, also the heat of CO adsorption decreases with CO coverage. Furthermore, the sticking coefficient of CO depends on the oxygen coverage in a temperature dependent fashion, which is attributed to CO precursor adsorption on

the oxygen covered surface. This is in agreement with previous published results on Pt(111) but not with data from Pd(111) and polycrystalline Pd. We think that this behavior may possibly be due to a structural phenomenon.

Acknowledgements

We thank Dr. Eva Hedborg for skilful sample preparation and Professor Ingemar Lundström for constructive criticism and constant support. This work was financed by the Swedish Natural Science Research Council (NFR) together with the Swedish Research Council for Engineering Sciences (TFR).

References

[1] I. Lundström, M. Armgarth, L.-G. Petersson, CRC Crit. Rev. Solid State Mater. Sci. 15 (1989) 201.
[2] M. Eriksson, L.-G. Ekedahl, Sensors and Actuators B42 (1997) 217.
[3] M. Eriksson, L.-G. Ekedahl, Appl. Surf. Sci. 133 (1998) 89.
[4] T. Engel, G. Ertl, J. Chem. Phys. 69 (1978) 1267.
[5] H. Conrad, G. Ertl, J. Küppers, Surf. Sci. 76 (1978) 323.
[6] G. Ertl, J. Koch, in: The Catalytic Oxidation of CO on Palladium Surfaces, North-Holland, Amsterdam, 1973, p. 969.
[7] J. Goschnick, J. Loboda-Cackovic, J.H. Block, M. Grunze, in: M. Grunze, H.J. Kreuzer (Eds.), Kinetics of Interface Reactions, vol. 8, Springer, Berlin, 1987, p. 269.
[8] T. Matsushima, J. Catal. 64 (1980) 38.
[9] C.T. Campbell, G.H. Ertl, H. Kuipers, J. Segner, J. Chem. Phys. 73 (1980) 5862.
[10] M. Eriksson, L.-G. Petersson, Surf. Sci. 311 (1994) 139.
[11] F. Nakao, Vacuum 25 (1975) 431.
[12] I. Lundström, M.S. Shivaraman, C. Svensson, J. Appl. Phys. 46 (1975) 3876.
[13] H.M. Dannetun, Linköping Studies in Science and Technology, Dissertations No. 160, Linköping University, Sweden, 1987.
[14] J. Fogelberg, Linköping Studies in Science and Technology, Dissertations No. 346, Linköping University, Sweden, 1994.
[15] L.-G. Petersson, H. Dannetun, I. Lundström, Surf. Sci. 161 (1985) 77.
[16] K. Wållberg, LiTH-IFM-EX-229, Linköping University, 1983.
[17] M. Milun, P. Pervan, K. Wandelt, Surf. Sci. 218 (1989) 363.
[18] C. Nyberg, C.-G. Tengstål, Surf. Sci. 126 (1983) 163.
[19] T. Matsushima, J.M. White, Surf. Sci. 67 (1977) 122.
[20] T. Engel, J. Chem. Phys. 69 (1978) 373.
[21] P.J. Kisliuk, J. Chem. Phys. 3 (1957) 95.
[22] P.J. Kisliuk, J. Chem. Phys. 5 (1958) 78.
[23] J. Goschnick, M. Grunze, J. Loboda-Cackovic, J.H. Block, Surf. Sci. 189/190 (1987) 137.
[24] E. Shustorovich, Surf. Sci. 176 (1986) L863.
[25] E. Shustorovich, Surf. Sci. 187 (1987) L627.
[26] B. Hellsing, V.P. Zhdanov, Chem. Phys. Lett. 147 (1988) 613.